Modular Organization of the PDZ Domains in the Human Discs-Large Protein Suggests a Mechanism for Coupling PDZ Domain-binding Proteins to ATP and the Membrane Cytoskeleton

Shirin M. Marfatia,* Joao H. Morais Cabral,‡ Lunhui Lin,* Colleen Hough,§ Peter J. Bryant,§ Lesley Stolz,‖ and Athar H. Chishti*

*Laboratory of Tumor Cell Biology, Department of Biomedical Research, St. Elizabeth's Medical Center, Tufts University School of Medicine, Boston, Massachusetts 02135; ‡Laboratory of X-Ray Crystallography, Dana Farber Cancer Institute, Harvard Medical School, Boston, Massachusetts 02115; §Developmental Biology Center, University of California, Irvine, California 92717; and ‖Pharmacia Biosensor, Cambridge, Massachusetts 02139

Abstract. The human homologue (hDlg) of the *Drosophila* discs-large tumor suppressor (Dlg) is a multidomain protein consisting of a carboxyl-terminal guanylate kinase-like domain, an SH3 domain, and three slightly divergent copies of the PDZ (DHR/GLGF) domain. Here we have examined the structural organization of the three PDZ domains of hDlg using a combination of protease digestion and in vitro binding measurements. Our results show that the PDZ domains are organized into two conformationally stable modules, one (PDZ^{1+2}) consisting of PDZ domains 1 and 2, and the other (PDZ^{3}) corresponding to the third PDZ domain. Using amino acid sequencing and mass spectrometry, we determined the boundaries of the PDZ domains after digestion with endoproteinase Asp-N, trypsin, and α-chymotrypsin. The purified PDZ^{1+2}, but not the PDZ^{3} domain, contains a high affinity binding site for the cytoplasmic domain of Shaker-type K^+ channels. Similarly, we demonstrate that the PDZ^{1+2} domain can also specifically bind to ATP. Furthermore, we provide evidence for an in vivo interaction between hDlg and protein 4.1 and show that the hDlg protein contains a single high affinity protein 4.1–binding site that is not located within the PDZ domains. The results suggest a mechanism by which PDZ domain–binding proteins may be coupled to ATP and the membrane cytoskeleton via hDlg.

THE complex of proteins underlying the plasma membrane is maintained, in large part, by high affinity interactions between specific protein domains. Variations in amino acid sequence between these domains can confer a high degree of specificity in these interactions, whereas the collection of a variety of such domains into multidomain polypeptides generates great complexity of the resulting assembly, known as the membrane cytoskeleton. This structure regulates cell shape, adhesion, and motility, and allows the organization of signal transduction pathways. The protein domain known as PDZ was initially identified as a 90–amino acid repeated motif in the synaptic junction protein, postsynaptic density protein (PSD)[1]-95/synapse-associated protein (SAP) 90 (Cho et al., 1992; Kistner et al., 1993). Three copies of the PDZ domain were identified in PSD-95 by virtue of a repeating GLGF signature sequence, and hence, this domain was originally named the GLGF repeat (Cho et al., 1992). However, since many similar domains in other proteins do not contain the GLGF signature sequence (Ponting and Phillips, 1995), they were renamed DHRs (discs large-homology region) to reflect their occurrence in the *Drosophila* discs-large tumor suppressor protein (Dlg) (Woods and Bryant, 1993). Dlg and rat PSD-95 are members of a recently discovered family of putative signaling proteins termed membrane-associated guanylate kinase homologues (MAGUKs), all of which contain DHRs. The family also includes human erythroid p55 (Ruff et al., 1991), the tight junction proteins Z0-1 and Z0-2 (Willot et al., 1993; Itoh et al., 1993; Jesaitis and Goodenough, 1994), a human homologue of Dlg (hDlg) (Lue et al., 1994), the product of the *dlg2* gene (Mazoyer et al., 1995), the prod-

Address all correspondence to Athar Chishti, St. Elizabeth's Medical Center, ACH4, 736 Cambridge Street, Boston, MA 02135. Tel.: (617) 789-3118. Fax: (617) 789-3111.

1. *Abbreviations used in this paper*: Dlg, *Drosophila* discs-large tumor suppressor protein; hDlg, human homologue of Dlg; GST, glutathione-*S*-transferase; GUK, guanylate kinase; MAGUK, membrane-associated guanylate kinase homologue; HE, hereditary elliptocytosis; PSD, postsynaptic density protein; RU, resonance unit; SAP, synapse-associated protein; TPCK, *N*-1-tosylamide-2-phenylethylchloromethyl ketone; 4.1^{N30}, 30-kD amino-terminal domain of protein 4.1.

uct of the *dlg3* gene (Smith et al., 1996), the *Caenorhabditis elegans* signaling protein, LIN2 (Hoskins et al., 1996), and CASK, which contains an amino-terminal calmodulin kinase fused with a dlg2-like protein (Hata et al., 1996). The rat homologue of hDlg has been cloned and reported as SAP97 (Müller et al., 1995). Recently, the DHR/GLGF domains have been renamed as PDZ (PSD-95/Discs large/ZO-1) domains to signify their presence in several proteins of distinct origin. We will use the nomenclature PDZ throughout the rest of this paper.

Sequence comparisons revealed variable number of PDZ domains in >30 proteins (Ponting and Phillips, 1995). A single copy is found in neuronal nitric oxide synthase, p55, dlg2, dlg3, LIN2, CASK, and syntrophin, whereas three copies are found in PSD-95, Dlg, hDlg, ZO-1, and ZO-2. The three PDZ domains within a single protein are designated PDZ^1, PDZ^2, and PDZ^3, respectively, starting from the amino-terminal end (Woods and Bryant, 1993). Other examples of proteins containing the PDZ domain include the *Drosophila* dishevelled protein (Klingensmith et al., 1993), the *C. elegans* signaling protein, LIN-7 (Simske et al., 1996), a subclass of protein tyrosine phosphatases, a protein with the leucine-zipper sequence, a chemoattractant factor, an LIM-kinase, and the *ros1* gene product from a glioblastoma cell line (Ponting and Phillips, 1995).

Recent findings indicate that the PDZ domains function as specific protein-recognition motifs. For example, one of the six PDZ domains present in the protein tyrosine phosphatase, FAP-1, mediates its binding to the cytoplasmic domain of the Fas cell surface receptor (Sato et al., 1995), and this binding is critical for Fas-induced apoptosis in T lymphocytes (Sato et al., 1995). Similarly, the PDZ^2 domain of PSD-95 binds to the cytoplasmic tail of the *N*-methyl-D-aspartate receptor (Kornau et al., 1995), and the PDZ^{1+2} domains of both PSD-95 and hDlg bind to the cytoplasmic domain of Shaker-type K^+ channels (Kim et al., 1995). The binding of PSD-95/hDlg with the *N*-methyl-D-aspartate receptors and K^+ channels may be involved in synaptic plasticity, and it appears to be necessary for the clustering of potassium channels expressed in heterologous COS cells (Kornau et al., 1995; Kim et al., 1995). Evidence for PDZ–PDZ domain associations was recently obtained by the demonstration that a single copy of the PDZ domain of neuronal nitric oxide synthase interacts with the PDZ domain of α-1-syntrophin (Brenman et al., 1996). Similarly, the PDZ domain of neuronal nitric oxide synthase interacts with the PDZ^2 domain of PSD-95 (Brenman et al., 1996). These results suggest that the PDZ domain plays a role in the subcellular localization of neuronal nitric oxide synthase. The functional significance of the PDZ domain was also demonstrated by the observation that a small deletion in the centrally located PDZ domain of the *Drosophila* dishevelled protein results in a phosphorylation-resistant protein that is inactive in the "Arm" assay (Yanagawa et al., 1995). More recently, Matsumine et al. (1996) have shown that the PDZ^2 domain of hDlg interacts with the carboxyl-terminal segment of adenomatous polyposis coli (APC) gene product. These findings indicate that the PDZ domains are novel protein modules that target cytoplasmic proteins to multiprotein complexes at the inner surface of the plasma membrane.

The characterization of hDlg protein began when our laboratory identified a high molecular weight band during immunoprecipitation of p55 protein from lysates of human B lymphocytes. The corresponding cDNA was subsequently cloned from a human B lymphocyte cDNA preparation using degenerate nucleotide primers based on the sequences of the cDNAs of PSD-95 and Dlg (Cho et al., 1992; Kistner et al., 1993; Woods and Bryant, 1991). The predicted primary structure of hDlg is similar to those of PSD-95 and Dlg except that the hDlg protein contains a novel amino-terminal segment that is not found in other MAGUKs (Lue et al., 1994). We have previously demonstrated that the hDlg protein binds to protein 4.1 in vitro (Lue et al., 1994). In this manuscript we show that the three PDZ domains of hDlg are organized into two protease-resistant modules. One module consists of PDZ domains 1 and 2, whereas the other contains PDZ domain 3. The PDZ^{1+2} module binds to ATP as well as to the cytoplasmic domain of Shaker-type K^+ channels. We also present evidence for the interaction of hDlg protein with protein 4.1 in vivo and show that protein 4.1 binds to hDlg at a single site outside of the PDZ domains.

Materials and Methods

hDlg Constructs

The cDNA constructs of full-length hDlg and the three PDZ domains (amino acids 201–584; PDZ^{1+2+3}) of hDlg, which were subcloned into pGEX-2T, have been described previously (Lue et al., 1994). The BamH1/EcoR1 fragment released from the PDZ^{1+2+3} cDNA construct in pGEX-2T was subcloned into the vector pRSETA. The cDNA construct expressing the PDZ^{1+2+3} protein attached to an amino-terminal His-tag fusion was transformed into *Escherichia coli* strain BL-21(DE3). The His–PDZ^{1+2+3} protein was purified as described (Invitrogen, San Diego, CA). cDNA fragments containing the PDZ^{1+2} domain (amino acids 201–464) and the PDZ^3 domain (amino acids 457–552) of hDlg were amplified using the primer pairs D12f/D12r and D3f/D3r, respectively. The primers containing the BamH1 or EcoR1 adaptors are as follows: D12f (sense, BamH1) 5′-CGCGGATCCCTGGTCAACACAGATA; D12r (antisense, EcoR1) 5′-CGGAATTCCAGGTTCCCTTGTAATT; D3f (sense, BamH1) 5′-CGCGGATCCGATGATGAAATTACA; D3r (antisense, EcoR1) 5′-CCGGAATTCACGACTGTATTCTTC. The PCR products were ligated into pGEX-2T vector and shown to express the expected size of glutathione-*S*-transferase (GST) fusion proteins in the *E. coli* DH5α cells. All the cDNA constructs were verified by DNA sequence analysis.

Drosophila Dlg Constructs

The cDNA fragments containing the three PDZ domains (amino acids 37–572) and PDZ^3 domain (amino acids 462–572) were amplified using the primer pairs: DHR1f (sense) 5′-TTATACGAGGACATTCAGCTGGAG; DHR3r (antisense) 5′-AAGCGATTGTACTCCTCTGG; and DHR3f (sense) 5′-AATGCTCTAGCCGCCGTTCC; DHR3r (antisense), respectively. The PCR products were first subcloned into the TA cloning vector pCR™II (Invitrogen), and then transferred into pGEX-4T-2 vector. The cDNA constructs expressed the expected size of GST fusion proteins in *E. coli* DH5α cells.

Protease Digestion of the Fusion Proteins

To investigate the modular organization of the PDZ domains of hDlg, purified His–PDZ^{1+2+3} fusion protein was digested with endoproteinase Asp-N (Boehringer Mannheim Biochemicals, Indianapolis, IN), *N*-1-tosylamide-2-phenylethylchloromethyl ketone (TPCK)–trypsin (Pierce Chemical Co., Rockford, IL) and α-chymotrypsin (Sigma Chemical Co., St. Louis, MO). The enzyme/protein ratio for Asp-N was 1:2,000 (wt/wt), for TPCK-trypsin 1:30 (wt/wt), and for α-chymotrypsin 1:83 (wt/wt). The His–PDZ^{1+2+3} protein was incubated with Asp-N for 2 h at room temperature in a buffer containing 50 mM Tris-HCl, pH 8.0, and 50 mM NaCl. Digestion with trypsin and α-chymotrypsin was carried out in the same buffer at

4°C, for overnight and 2 h, respectively. The protease-resistant PDZ^{1+2} and PDZ^3 domains thus produced were purified by gel filtration on a Superdex 75 column (Pharmacia Biotech, Piscataway, NJ) followed by chromatography on a Mono-Q anion exchange column (Pharmacia Biotech). For all subsequent biochemical studies, the PDZ^{1+2} domain was obtained from the GST–PDZ^{1+2} fusion protein by digestion with trypsin and α-chymotrypsin. The immobilized GST–PDZ^{1+2} fusion protein was first cleaved with thrombin (Smith and Johnson, 1988). The released PDZ^{1+2} fragment was then digested with either TPCK-trypsin or α-chymotrypsin to produce either PDZ^{1+2} (T) or PDZ^{1+2} (C), respectively. Amino-terminal sequencing and mass spectrometric analysis of PDZ^{1+2} and PDZ^3 domains were carried out according to standard procedures. For low angle rotary-shadowing EM, the His–PDZ^{1+2+3} and PDZ^{1+2} (T) proteins were sprayed onto freshly cleaved mica in the buffer containing 70% glycerol. Rotary shadowing was performed with platinum-carbon and carbon anodes, and floated replicas were mounted on 400-mesh copper grids (Tyler et al., 1980).

Preparation of ^{125}I-labeled 30-kD Domain of Protein 4.1

Native protein 4.1 was isolated from human RBCs using the procedure of Ohanian and Gratzer (1984). The 30-kD amino-terminal domain of protein 4.1 (4.1^{N30}) was obtained by limited digestion of pure protein 4.1 with α-chymotrypsin at an enzyme/substrate ratio of 1:25. The protease digestion was carried out on ice in a buffer containing 10 mM Tris-HCl, pH 8.0. After incubation for 90 min, the enzyme activity was quenched with 4.0 mM diisopropyl fluorophosphate. The digested material was fractionated on a Mono-Q column using a linear gradient of 20–500 mM sodium chloride. The purified 4.1^{N30} domain was then radiolabeled with ^{125}I-labeled Bolton-Hunter reagent (Ling et al., 1988).

Synthetic Peptides

The positively charged cluster of amino acids located between the PDZ^1 and PDZ^2 domains of hDlg (YVKRRKPVSEKIMEIKLIK; peptide C) was chemically synthesized. Another synthetic peptide corresponding to the COOH terminus of the Kv1.4 potassium channel (DKNNCSNAKAVETDV) was coupled to biotin at the amino terminus via an inert spacer sequence, SGSG. The synthetic peptides were purified by high pressure liquid chromatography on an analytical reverse phase column, and the purity of the peptides was confirmed by amino acid analysis and mass spectrometry.

Sedimentation Assay

The purified GST fusion proteins bound to glutathione beads (5.0 μg/50 μl of 50% bead suspension) were incubated with ^{125}I-4.1^{N30} domain in binding buffer containing 5.0 mM sodium phosphate, pH 7.6, 1.0 mM β-mercaptoethanol, 0.5 mM EDTA, 120 mM potassium chloride, 0.02% sodium azide, and 1.5 mg/ml of BSA (binding buffer). The total volume of the reaction mixture was 500 μl. After incubation at 4°C for 90 min with slow mixing, the beads were washed thoroughly with the binding buffer to remove the unbound ^{125}I-4.1^{N30}. The bound radioactivity was measured in a γ-counter. For competition experiments, molar excess of either PDZ^{1+2} or peptide C was preincubated with ^{125}I-4.1^{N30} in the binding buffer at 4°C for 60 min, followed by the addition of GST fusion proteins bound to the beads. The beads were incubated for 90 min with slow mixing at 4°C. To study the effect of K^+ channel peptide on the interaction between hDlg and ^{125}I-4.1^{N30}, the GST–hDlg fusion protein on beads was preincubated with molar excess of the Kv1.4 peptide for 60 min before the addition of ^{125}I-4.1^{N30}. For Scatchard analysis, the binding data were obtained by incubating increasing amounts of ^{125}I-4.1^{N30} with a fixed amount of GST–hDlg fusion protein in the binding buffer described above. To determine the contribution of nonspecific binding of ^{125}I-4.1^{N30}, a parallel control of GST was included for each concentration of ^{125}I-4.1^{N30}.

ATP-binding Assay

This assay was carried out by incubation of the purified protein in solution with [γ-^{32}P]ATP (100–500 nCi) and 100 nM of cold ATP in an ATP-binding buffer (10 mM Hepes, pH 7.6, 50 mM KCl, 75 mM NaCl, 1.0 mM $MgCl_2$, 1.0 mM EGTA, 1 mM β-mercaptoethanol, and 0.02% NaN_3). After incubation on ice for 3 h, the reaction mixture (150 μl) was applied to a prewetted nitrocellulose filter (HA-type, 0.45 μm; Millipore Corp., Redford, MA). After washing the filter extensively with ATP-binding buffer, the radioactivity bound to the filter was counted in a scintillation counter. The concentration of cold ATP was determined by absorbance at 259 nm.

The GST fusion proteins were eluted from the glutathione beads with 5.0 mM reduced glutathione in the elution buffer containing 75 mM Hepes, pH 7.6, 150 mM NaCl, 5.0 mM DTT, 0.1% Triton X-100, and protease inhibitors. The eluted proteins were extensively dialyzed against the ATP-binding buffer before use in the ATP-binding assay. Appropriate controls of GST or BSA were included to measure nonspecific binding. A Millipore-1225 sampling manifold apparatus was used to process protein samples either in duplicate or triplicate. The Scatchard plot was generated by incubating 2.0 μg of the GST–PDZ^{1+2+3} protein with increasing concentrations of ATP. A parallel GST control was included for each ATP concentration. Each presented result is an average of duplicate determinations.

Surface Plasmon Resonance Measurements

The BIAcore and Fisons IASys instruments (Pharmacia Biosensor, Piscataway, NJ) use surface plasmon resonance phenomenon to measure interactions. Surface plasmon resonance is used to probe the refractive index change in a flow cell due to the binding of molecules to immobilized ligand. Light impinging on a gold surface between layers with two different refractive indices resonates with outer shell electrons, resulting in a decrease in reflected light intensity under conditions of total internal reflection. Protein mass determines refractive index regardless of the amino acid sequence; therefore, the change in light intensity is directly proportional to the protein mass bound to the ligand. In a typical experiment, the ligand is immobilized to the chip surface, and the analyte is passed over the bound ligand. An interaction between ligand and analyte results in an increase of mass at the chip surface. The signal is recorded as resonance units (RU). A change of 1,000 RU corresponds to a change in protein surface concentration of ~1.0 ng/mm^2. A plot of RU vs time (sensogram) consists of an association phase, an equilibrium phase, and a dissociation phase. To measure the interaction of K^+ channel peptide with the PDZ domains of hDlg, 28.0 RU of biotinylated Kv1.4 peptide was immobilized on a streptavidin surface (see Fig. 6 *A*). In Fig. 6 *B*, 1,200 RU of GST–PDZ^{1+2+3} protein was immobilized on a surface coated with 6,000 RU of polyclonal anti-GST antibodies.

Results

The PDZ Domains of hDlg Are Organized into Two Protease-resistant Modules

A histidine-tag fusion protein (PDZ^{1+2+3}) was produced that contained all three PDZ domains along with flanking sequences (residues Leu 201 to Leu 584; Figs. 1 and 2). A comparison of the molecular mass of PDZ^{1+2+3} fusion protein by gel filtration (69 kD) with the calculated value of 45.2 kD (Table I) suggested some asymmetry in the shape of the purified PDZ^{1+2+3} fusion protein. To test whether this asymmetry may be a consequence of conformationally distinct organization within the three PDZ domains, the purified PDZ^{1+2+3} protein was incubated with low concentrations of endoproteinase Asp-N (1:2,000 wt/wt). Limited proteolysis cleaved the three PDZ domains of hDlg into two Coomassie-stainable bands of 28 and 10 kD, which migrated as 33- and 12-kD polypeptides, respectively, on a gel filtration column (Table I; Fig. 1 *B*). The boundaries of the two polypeptides were determined by amino-terminal sequencing and matrix-assisted laser desorption mass spectrometry. The amino terminus of the 33-kD polypeptide obtained by Asp-N cleavage starts at aspartic acid-205, whereas the carboxyl terminus was calculated to be asparagine-411 from the molecular mass determined by mass spectrometry. The 33-kD polypeptide therefore includes PDZ domains 1 and 2 as well as 20 amino acids of flanking sequence located at the amino terminus of PDZ domain 1. It is relevant to mention here that when PDZ^{1+2} domain is obtained by digestion of corresponding GST fusion protein with trypsin and chymotrypsin, two amino acids from

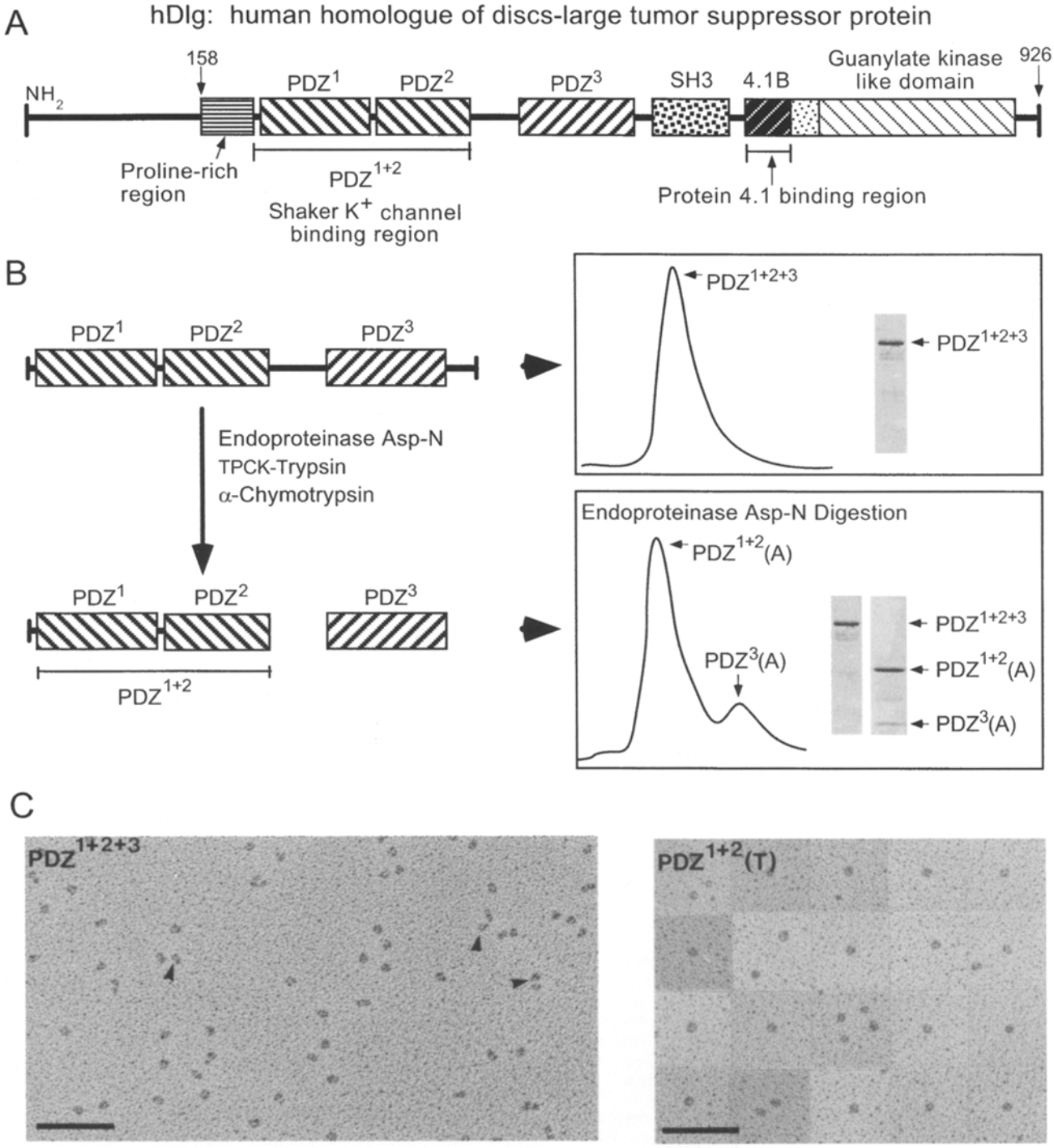

Figure 1. Characterization of the PDZ domains of hDlg. (*A*) Schematic representation of hDlg protein showing various protein domains. The proline-rich region and the protein 4.1–binding domain (*4.1B*) are encoded by alternatively spliced exons that were originally designated as insertions I^1 and I^3, respectively (Lue et al., 1994). (*B*) The His–PDZ^{1+2+3} fusion protein of hDlg was digested with either endoproteinase Asp-N (A), TPCK-trypsin (T), or α-chymotrypsin (C). The approximate location of protease-resistant domains, PDZ^{1+2} module and PDZ^3, is shown in the left panel. The right panel shows the elution profile and SDS-PAGE analysis of the three proteins. The sizes of the His–PDZ^{1+2+3} fusion protein (69 kD), the PDZ^{1+2} (A) module (33 kD), and the PDZ^3 (A) domain (12 kD) were determined by gel filtration on a Superose 12 column. The following protein markers were used: cytochrome C (12,000), carbonic anhydrase (29,000), BSA (66,000), β-amylase (200,000), and thyroglobulin (669,000). See Table I for complete listing of the molecular mass of various protein domains. (*C*) Electron micrographs of low angle rotary-shadowed replicas of His–PDZ^{1+2+3} fusion protein and PDZ^{1+2} (T) module. (*Arrowheads*) Elongated morphology of His–PDZ^{1+2+3} molecules as compared with the globular shape of PDZ^{1+2} (T). Bar, 0.1 μm.

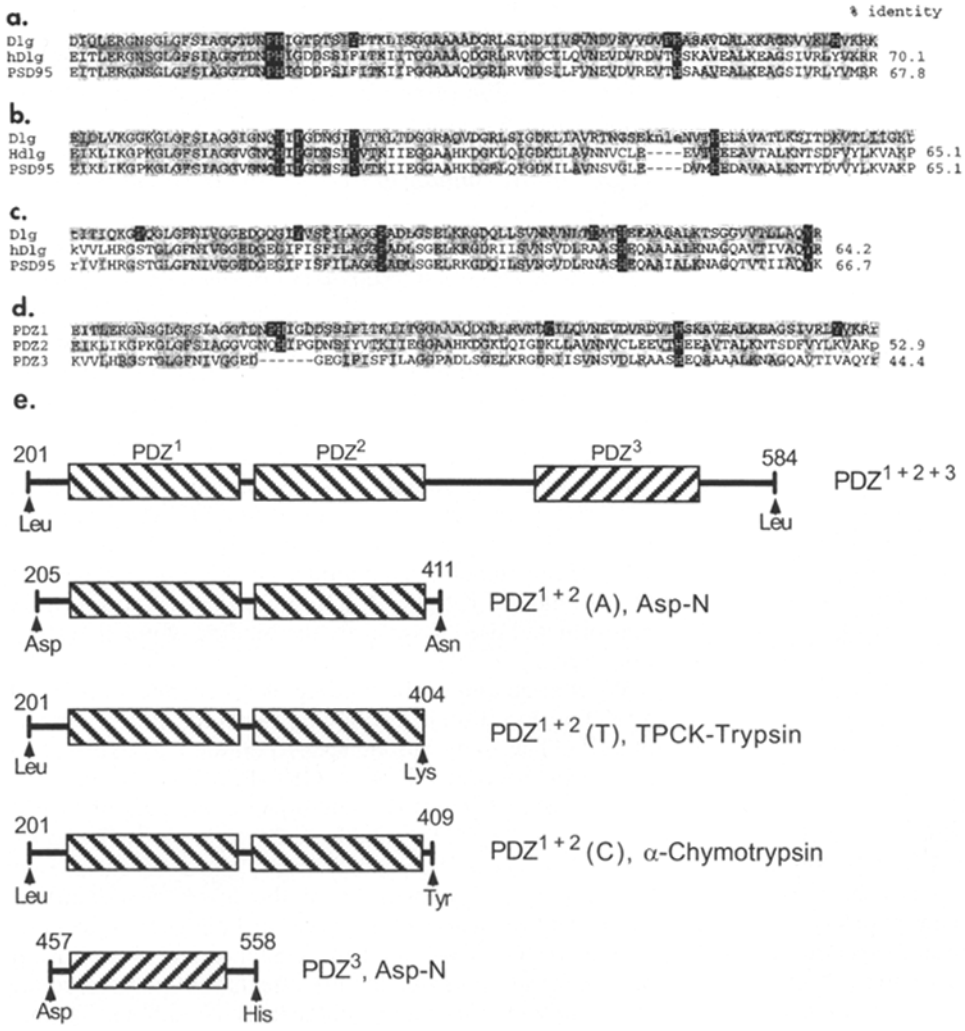

Figure 2. Sequence alignment of the PDZ domains. The sequences were aligned using the MACAW program, which highlights matching amino acids such as proline, histidine, and tyrosine with a darker shade. (*a*, *b*, and *c*) PDZ domains 1, 2, and 3, respectively. (*d*) A comparison of three PDZ domains in hDlg. (*e*) Schematic representation of the protease-resistant PDZ domains of hDlg.

the carboxyl end of GST are added to the amino terminus of PDZ^{1+2} domain (Table I). Similarly, the amino and carboxyl termini of the 12-kD polypeptide were determined to be aspartic acid-457 and histidine-558, respectively (Table I). The boundaries of the 12-kD polypeptide correspond to those of PDZ domain 3, without any flanking sequence (Fig. 1 *B*). It is noteworthy here that the PDZ^3 domain in solution migrates as a dimer (18 kD) at high protein concentrations (≥1.5 mg/ml). Both trypsin and chymotrypsin cleaved the PDZ^{1+2+3} protein into two modules that are similar but not identical to those produced by Asp-N. The amino acids corresponding to the boundaries of PDZ^{1+2} domain released by trypsin and chymotrypsin are shown in Table I.

In summary, the three PDZ domains of hDlg are organized into two protease-resistant modules. The PDZ^{1+2} module includes PDZ domains 1 and 2 and 20–23 amino acids upstream of PDZ domain 1 (Table I). In contrast, the PDZ^3 domain is released as an independent module without a significant contribution from the flanking sequences. Low angle rotary shadow images indicate a relatively globular shape of the PDZ^{1+2} module as compared with the PDZ^{1+2+3} protein (Fig. 1 *C*).

A Subset of PDZ Domains Are ATP-binding Protein Modules

While studying the guanylate kinase activity of hDlg, we observed that GST fusion protein containing either full-length hDlg or PDZ^{1+2+3} domains bound ATP. The binding of radiolabeled ATP to the fusion protein in solution was quantified using a filter binding assay similar to one previously used to measure ATP binding to dematin and protein 4.2 (Azim et al., 1996). As shown in Fig. 3 *A*, ATP bound to purified GST-hDlg protein (26 mmol/mol) and GST-PDZ^{1+2+3} protein (22 mmol/mol). We then examined binding specificity within the three PDZ domains of hDlg. The PDZ^{1+2} domains, which were prepared by cleavage of the GST fusion protein using thrombin/chymotrypsin/trypsin, showed a comparable level of binding activity (1.3 mmol/mol), whereas the PDZ^3 domain of hDlg was inactive for ATP binding (Fig. 3 *B*). The relatively lower binding capacity of PDZ^{1+2} as compared with GST–PDZ^{1+2+3} might be due to a partial inactivation of PDZ^{1+2} during enzymatic cleavage and subsequent purification, or to having a more stable conformation as a fusion protein. The in vitro binding of ATP also occurred with a

Table I. Characterization of Recombinant hDlg Proteins

hDlg constructs	Amino acid boundaries*	Molecular mass (kD) Calculated‡	SDS-PAGE	Gel filtration
His-PDZ^{1+2+3}	LVN–RSL (201–584)	45.2§	44	69
PDZ^{1+2}(A)	DSL–YMN (205–411)	22.3	28	33
PDZ^{3}(A)	DDE–KIH (457–558)	10.9	10	12**
PDZ^{1+2} (thrombin cleaved)	LVN–REP (201–464)	29.1‖¶	36	ND
PDZ^{1+2}(T)‡‡	LVN–PAR (201–446)	26.5‖	33	ND
PDZ^{1+2}(T)§§	LVN–VAK (201–404)	22.1‖	28	ND
PDZ^{1+2}(C)	LVN–SMY (201–409)	22.6‖	28	ND

*The carboxyl terminus was determined by mass spectrometry measurements.
‡The calculated values were obtained using MacVector computer program.
§Molecular mass includes 4,147 daltons, contribution from the 36 amino acids of His-tag.
‖Molecular mass includes 180 daltons, contribution of glycine and serine residues from the carboxyl terminus of GST.
¶Molecular mass also includes five amino acids (G, I, H, R, D: 668 daltons) from the pGEX-2T before the stop codon.
**PDZ^{3}(A) domain migrates as dimer at high protein concentrations.
‡‡TPCK-trypsin to protein ratio of 1:30 (wt/wt) at 4°C.
§§TPCK-trypsin to protein ratio of 1:20 (wt/wt) at room temperature.
A, *T*, and *C*, Asp-N, TPCK-trypsin, and α-chymotrypsin, respectively.

Drosophila Dlg GST–PDZ^{1+2+3} fusion protein (Fig. 3 *C*). It should be noted that the Dlg GST–PDZ^{1+2+3} fusion protein is highly unstable despite necessary precautions, and therefore complicates the measurement of protein concentration required for precise calculation of specific activity. Nevertheless, the nucleotide-binding activity of the PDZ domains was specific for ATP since no binding was detected with the radiolabeled GTP (data not shown). In addition, the binding of labeled ATP to fusion proteins failed in competition with a large excess of cold, nonlabeled ATP, but it succeeded when competing with an excess of cold, nonlabeled GTP. The binding of ATP to the GST–PDZ^{1+2+3} fusion protein of hDlg is saturable and of high affinity with a K_d value of 6.5 ± 1.3 nM (Fig. 4).

High Affinity Binding of PDZ^{1+2} Module to Shaker-type K$^+$ Channels

Using a yeast two-hybrid screen, Kim et al. (1995) have recently shown that the distal end of the cytoplasmic domain of Shaker-type K$^+$ channels interacts with the PDZ domains 1 and 2 of hDlg and PSD-95. Here we have used surface plasmon resonance technology to quantify the interaction of K$^+$ channels with the PDZ domains of hDlg. A synthetic peptide, DKNNCSNAKAVETDV, modeled after the carboxyl-terminal 15 amino acids of voltage-gated Shaker-type K$^+$ channel Kv1.4 was coupled to biotin at the amino terminus. A spacer arm of SGSG was introduced between biotin and the peptide to provide adequate flexibility of the immobilized peptide. The biotinylated peptide of K$^+$ channel Kv1.4 was immobilized on a streptavidin platform and used to quantify the binding of purified PDZ domains.

We first measured the binding of K$^+$ channel peptide to a GST fusion protein containing the three PDZ domains of hDlg. The immobilized Kv1.4 peptide was exposed to increasing concentrations of GST–PDZ^{1+2+3} fusion protein (25 nM to 400 nM), yielding an overall K_d of 11 nM ($k_a = 1.8 \times 10^5\ M^{-1}s^{-1}$ and $k_d = 2.0 \times 10^{-3}s^{-1}$) (BIAcore 1000; Pharmacia Biosensor) (Fig. 5 *A*). It is clear from both the dissociation phase of the lower concentration curves and the association phase of the higher concentration curves (Fig. 5 *A*) that the GST portion of the fusion protein is causing some avidity effects that may influence the affinity measurements under these conditions. To correct this error, we reversed the orientation of the binding experiment by immobilizing the GST–PDZ^{1+2+3} fusion

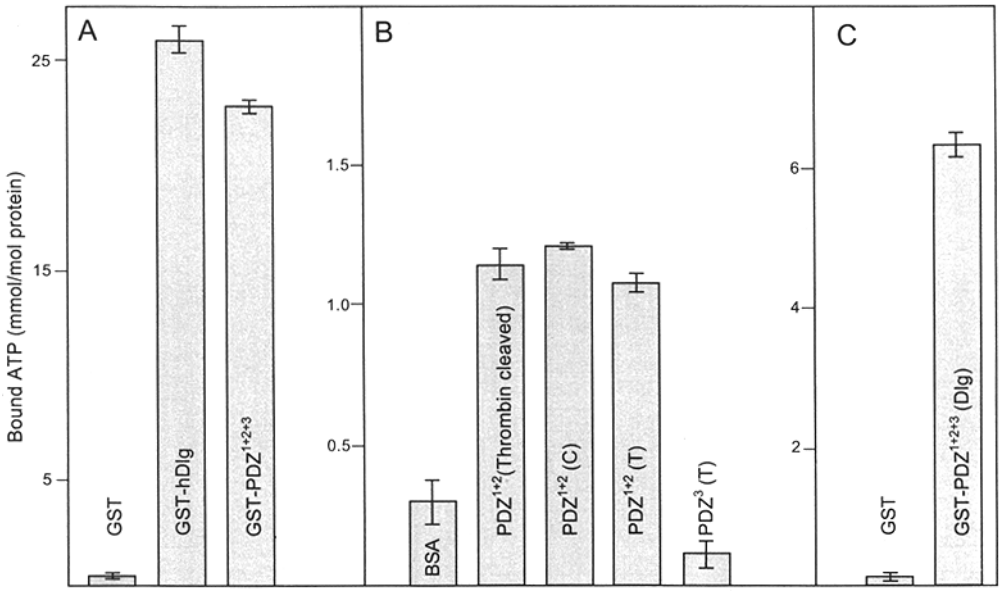

Figure 3. Binding of ATP to the recombinant fusion proteins of hDlg and Dlg. The ATP binding was measured using a solution-binding assay as described in Materials and Methods. (*A*) Binding of ATP to the full-length GST–hDlg and GST–PDZ^{1+2+3} fusion proteins. (*B*) Binding of ATP to the protease-resistant PDZ^{1+2} domain and PDZ^{3} domain of hDlg. These domains were obtained by cleavage of the His–PDZ^{1+2+3} fusion protein with trypsin, PDZ^{1+2} (T), and chymotrypsin, PDZ^{1+2} (C). The thrombin-cleaved PDZ^{1+2} domain was obtained from GST–PDZ^{1+2} fusion protein. (*C*) Binding of ATP to the GST–PDZ^{1+2+3} fusion protein of Dlg. Note that the rapid degradation of Dlg fusion protein prevented accurate determination of protein concentration. Error bars represent SEM (n = 3/4). The details of the proteins used for ATP binding are described in Materials and Methods.

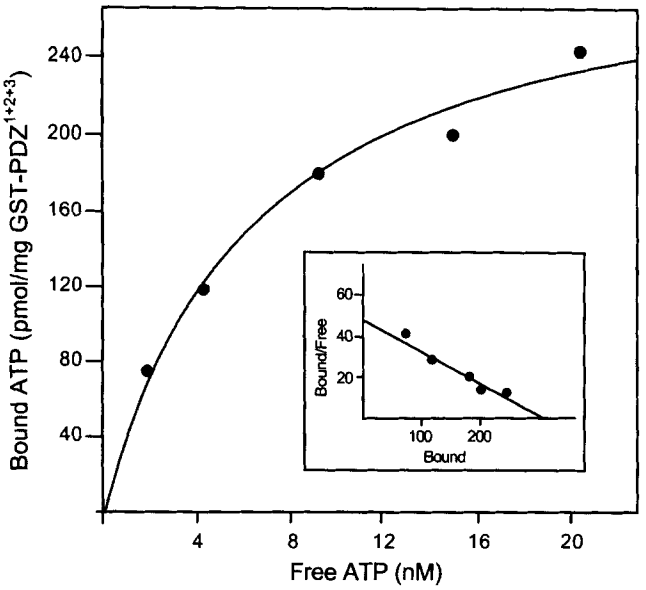

Figure 4. Quantification of ATP binding to the GST–PDZ^{1+2+3} fusion protein of hDlg. The details of the ATP-binding assay are described in Materials and Methods. The binding parameters were calculated using ENZFITTER (Elsevier-BIOSOFT, copyright 1987) program. The Scatchard analysis (*inset*) indicated the presence of a single class of binding sites with a K_d value of 6.5 ± 1.3 nM. Each value is an average of duplicate determinations that were within 10% of experimental variation. It should be noted that Kistner et al. (1995) have recently shown that the GST–SAP90 fusion protein (full-length) binds ATP in the millimolar range. They have used a solid phase ATP-binding assay by immobilizing the GST fusion protein to agarose beads. Whether the high affinity binding of ATP to PDZ domains of hDlg reflects a consequence of in-solution binding or a sequence-specific difference remains to be determined.

protein on the biosensor chip coated with polyclonal antibodies against GST (BIAcore 2000; Pharmacia Biosensor) (Fig. 5 *B*). The Kv1.4 peptide was injected at concentrations ranging from 0.31–5.0 μM. The kinetic constants that were obtained from this experiment were: $k_a = 1.5 \times 10^5$ $M^{-1}s^{-1}$ and $k_d = 2.4 \times 10^{-2}s^{-1}$, giving an overall $K_d = 160$ nM. A distinctive feature of the results is a significant change in the dissociation rate when the orientation of the experiment is reversed (Fig. 5 *B*). The on-rate is virtually identical to that shown in Fig. 5 *A*; however, the off-rate is 10-fold faster, illustrating the potential contribution of GST dimerization to the off-rate (Fig. 5 *B*). No binding of Kv1.4 peptide was detected with the GST alone. We also measured the binding of immobilized Kv1.4 peptide to PDZ domains 1 and 2 without the GST fusion protein. The PDZ^{1+2} module and the PDZ^3 domain of hDlg were produced by Asp-N digestion. As shown in Fig. 6 *A*, the Kv1.4 peptide binds to PDZ^{1+2} module with high affinity. A K_d value of 33 ± 5 nM was calculated from the association ($k_a = 4.13 \times 10^5$ $M^{-1}s^{-1}$) and dissociation ($k_d = 0.0135$ s^{-1}) rate constants (Fig. 6, *B* and *C*; Fisons IAsys instrument). The PDZ^3 domain of hDlg did not bind to the immobilized Kv1.4 peptide (Fig. 6 *A*). Finally, we examined whether the binding of ATP to GST–PDZ^{1+2+3} fusion protein can modulate its interaction with the Kv1.4 peptide. No effect on the binding affinity was observed in the presence of either 0.5 or 2.0 mM ATP–Mg^{+2} complex (data not shown).

The Protein 4.1-binding Site Is Not Located within the PDZ Domains of hDlg

We have previously shown that the 4.1^{N30} domain binds to p55 and hDlg within a positively charged domain located between the SH3 and guanylate kinase-like domains (Marfatia et al., 1995). The protein 4.1–binding site in hDlg is encoded by an alternatively spliced insertion termed I^3 or 4.1B (Lue et al., 1994; Marfatia et al., 1995). In addition, we have previously shown that protein 4.1 can also bind to a fusion protein containing the three PDZ domains of hDlg (Lue et al., 1994). However, the binding measurements indicated that protein 4.1 binds to the three PDZ domains of hDlg with significantly lower affinity as compared with its binding within the 4.1B (I^3) domain (Lue et al., 1994). To resolve the issue of the number of protein 4.1–binding sites within hDlg, we searched for 4.1-binding insert (I^3)–like sequences within the primary structure of hDlg. The sequence alignment revealed a positively charged cluster of amino acids at the interface of PDZ domains 1 and 2 (see peptide C). We used several experimental approaches to test whether the observed interaction between protein 4.1 and the PDZ domains of hDlg may be an artifactual consequence of these positively charged amino acids. First, the binding measurements were conducted using native protein 4.1, which was purified from human RBC membranes. The 4.1^{N30} domain was obtained by proteolytic digestion of purified protein 4.1, thus eliminating factors that may influence the activity of protein 4.1 produced by in vitro translation systems (Lue et al., 1994; Pelham and Jackson, 1976). As shown in Fig. 7 *A*, the GST–PDZ^{1+2+3} fusion protein of hDlg sedimented 38% of protein 4.1 as compared with the binding of protein 4.1 to full-length GST–hDlg fusion protein. To further investigate the protein 4.1–binding site within the three PDZ domains of hDlg, a 19–amino acid peptide (peptide C) was synthesized that included the positively charged amino acid cluster located between the PDZ domains 1 and 2. The peptide C did not affect the binding of protein 4.1 to the GST-hDlg and GST–PDZ^{1+2+3} fusion proteins even at molar concentrations vastly in excess of the respective fusion proteins (Fig. 7 *A*). Next, we examined whether the PDZ^{1+2} module, which contains PDZ domains 1 and 2 including the positively charged cluster of amino acids, can inhibit the binding of protein 4.1 to GST–hDlg fusion protein. Again, no effect on binding was observed irrespective of whether the PDZ^{1+2} module was produced by chymotrypsin or trypsin (Fig. 7 *B*). Consistent with these findings, no binding between protein 4.1 and the PDZ^{1+2} module was detected by a blot overlay assay (data not shown).

We also examined whether the presence of Kv1.4 peptide can modulate the binding of protein 4.1 to hDlg. The PDZ^{1+2} module released by trypsin cleavage was incubated with the biotinylated Kv1.4 peptide that was coupled to the streptavidin beads. The unbound PDZ^{1+2} module was removed by repeated washings of the beads. The presence of PDZ^{1+2} module bound to streptavidin beads is shown in the inset of Fig. 7 *C*. The PDZ^{1+2} module bound

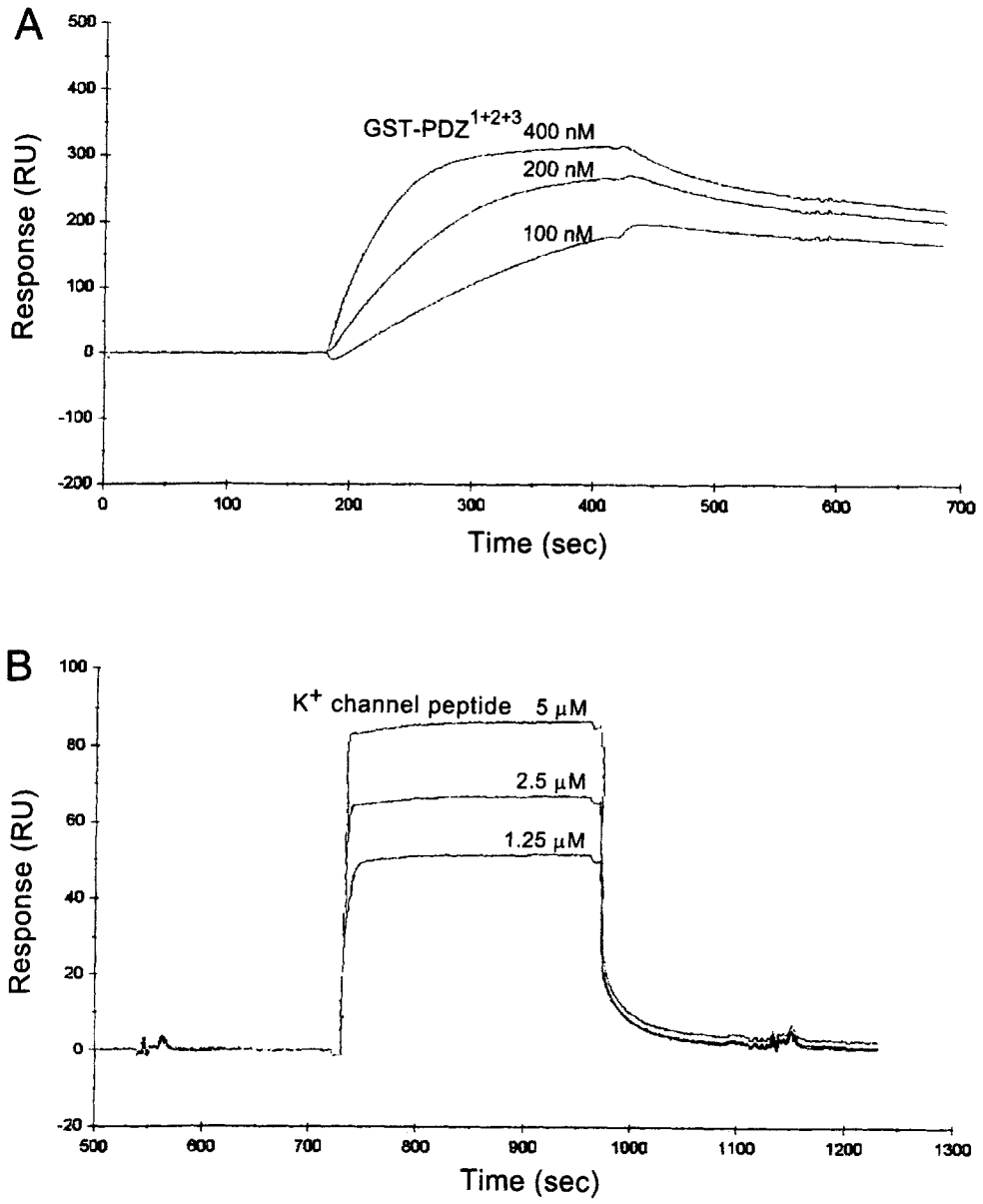

Figure 5. Interaction between K^+ channel peptide and the GST–PDZ^{1+2+3} fusion protein of hDlg. (*A*) The Kv1.4 channel peptide was immobilized on the streptavidin chip, and the binding of GST–PDZ^{1+2+3} fusion protein was measured at increasing concentrations of the fusion protein (BIAcore 1000; Pharmacia Biosensor). K_d = 11 nM. (*B*) The GST–PDZ^{1+2+3} fusion protein was immobilized on the chip coated with anti-GST antibodies. The binding of Kv1.4 channel peptide was measured at increasing concentrations of the peptide (BIAcore 2000). K_d = 160 nM. It should be noted that only the data from three out of five concentrations are shown in *A* and *B*. The rates were calculated using nonlinear regression techniques so that the shapes of the curves for the association phase will look different because of the different off-rates between the two experimental designs. The change in off-rates during the dissociation phase between the two experimental designs is a clear indication of the avidity effects caused by the dimerization of the GST fusion proteins.

to Kv1.4 peptide was then tested for binding to the 4.1^{N30}, but no binding was detected (Fig. 7 *C*). Similarly, molar excess of Kv1.4 peptide had no effect on the binding of protein 4.1 to GST–hDlg fusion protein (Fig. 7 *D*). Finally, to further support our contention that there is only one binding site for protein 4.1 in hDlg, we analyzed the binding of protein 4.1 to GST–hDlg fusion protein by Scatchard analysis. As shown in Fig. 8, protein 4.1 binds to hDlg at a single class of high affinity binding sites characterized with a K_d of 5.3 ± 0.4 nM. Based on these data, we conclude that the binding of protein 4.1 to hDlg is mediated by an alternatively spliced exon (4.1 binding insert) that is located between the exons of SH3 and guanylate kinase (GUK) domains.

Evidence for Interaction between hDlg and Protein 4.1 In Vivo

The hDlg transcript and hDlg immunoreactive polypeptides are found in many cells and tissues (Lue et al., 1994; our unpublished data). Using an affinity-purified antibody against human lymphocyte hDlg, the hDlg protein was detected in human RBC membranes (Fig. 9, lane 2). Western blotting revealed a major immunoreactive polypeptide of 80 kD and a minor immunoreactive band of ~125 kD (Fig. 9, lane 2, *arrowhead* and *asterisk*). The presence of two immunoreactive forms of hDlg in the red cell membrane is consistent with our previous findings documenting the presence of multiple transcripts of hDlg in human B lymphocytes (Lue et al., 1994). The two polypeptides of hDlg protein in the red cell membrane may be encoded by the alternatively spliced transcripts derived from a single copy of the *hDlg* gene on chromosome 3 (Azim et al., 1995). To test whether the presence of protein 4.1 is required to retain all forms of hDlg on the membrane, we examined the presence of hDlg protein in the membranes of RBCs from a patient with protein 4.1 (−) hereditary elliptocytosis (HE). The primary genetic defect in 4.1(−) HE involves

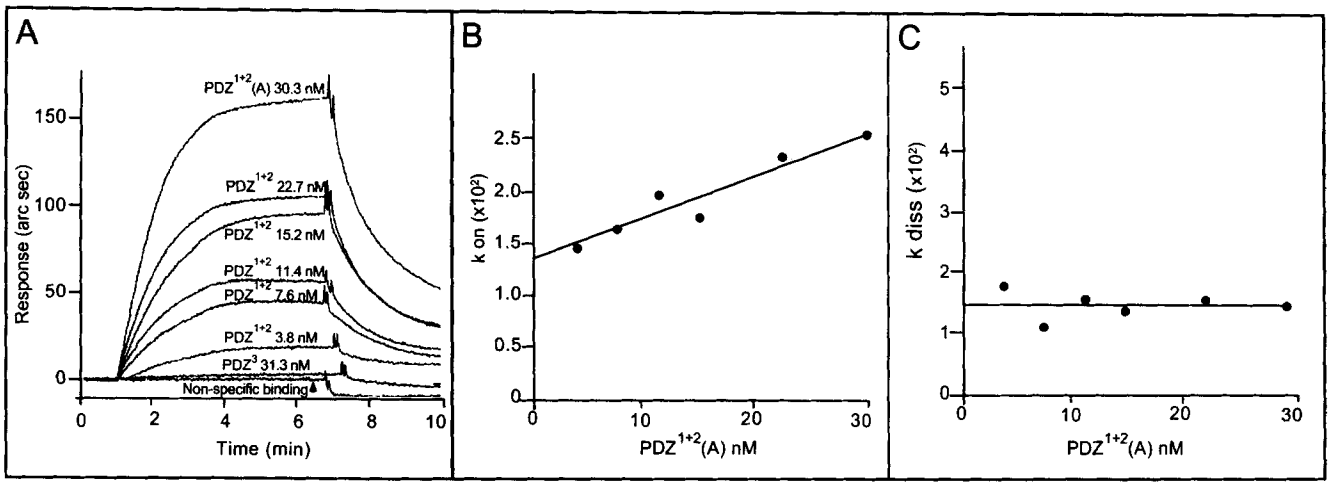

Figure 6. Interaction of PDZ^{1+2} (A) module of hDlg with the K^+ channel (Kv1.4) peptide. The binding was quantified using Fisons IAsys Biosensor machine. Biotinylated Kv1.4 peptide was immobilized onto a streptavidin platform, and increasing concentrations of PDZ^{1+2} (A) protein were passed over the immobilized peptide. (*A*) The overlay plot showing specific association and dissociation phases generated at increasing concentrations of PDZ^{1+2} (A). Nonspecific binding contribution was determined by passing PDZ^{1+2} (A) protein over a nonspecific protein immobilized onto the streptavidin platform. (*B*) Plot of observed on-rate vs protein concentration in nM. The slope of the plot gives the association rate constant ($k_a = 4.13 \times 10^5\ M^{-1}s^{-1}$), and the intercept on the y-axis gives the dissociation rate constant ($k_d = 0.0135\ s^{-1}$). (*C*) Plot of fitted dissociation rate vs protein concentration in nM. The intercept on the y-axis gives the dissociation rate constant ($k_d = 0.0149\ s^{-1}$). The dissociation constant (K_d) was calculated to be 33 ± 5 nM, indicating a high affinity interaction between Kv1.4 channel peptide and PDZ^{1+2} (A) protein. As expected, the observed on-rate increases linearly with an increase in the PDZ^{1+2} protein concentration (*B*), whereas the dissociation rate remains constant (*C*).

protein 4.1 and results in elliptocytosis of RBCs and hemolytic anemia (Feo et al., 1980). The membranes of protein 4.1 (−) HE RBCs completely lack all forms of protein 4.1 and show a secondary loss of p55 and glycophorin C (Alloisio et al., 1993; Chishti et al., 1996). The hDlg protein was also completely missing from the membranes of protein 4.1 (−) HE RBCs (Fig. 9, lane *3*). The concomitant loss of protein 4.1 and hDlg from the membranes of 4.1 (−) HE RBCs provides the first evidence for the in vivo association between hDlg and protein 4.1 in a mammalian cell.

Previously, we have proposed that the hDlg protein may interact with members of the protein 4.1 superfamily like ezrin and PTP-H1 whose amino termini are very similar to the 30-kD domain of protein 4.1 (Lue et al., 1994). First, we tested the binding of hDlg with native ezrin that was purified from human placenta. The immobilized GST–hDlg fusion protein failed to bind to purified ezrin as well as ezrin in lysates of HeLa cells (data not shown). Furthermore, we detected normal amounts of ezrin in the RBC membranes of a patient with protein 4.1 (−) HE (Fig. 9, lane *4*). Since the protein 4.1 (−) HE RBCs do not contain either hDlg or p55, we conclude that the hDlg protein does not directly bind to ezrin in vivo. Similarly, no interaction of GST–hDlg protein was detected with the tyrosine phosphatase, PTP-H1, which was expressed in the baculovirus expression system (data not shown). In summary, our results indicate that protein 4.1 specifically binds to the hDlg protein both in vitro and in vivo.

Discussion

This investigation was undertaken to elucidate the structural and functional role of PDZ domains in hDlg, the human homologue of the *Drosophila* discs-large tumor suppressor protein. Our results show that the three PDZ domains of hDlg are organized into two protease-resistant conformationally stable modules. The PDZ domains 1 and 2 are contained within a single protease-resistant module, which also includes 20 amino acids located at the amino terminus of PDZ domain 1 (Fig. 1). In contrast, the protease treatment released the PDZ^3 domain as an independent module without the flanking sequences. The presence of a protease-resistant PDZ^{1+2} module is consistent with the closely apposed location of the PDZ domains 1 and 2 in the hDlg sequence (Fig. 1). Indeed, a 53% sequence identity between PDZ domains 1 and 2 of hDlg suggests that the two domains may belong to a subclass that is distinct from the PDZ^3 domain; both PDZ domains 1 and 2 are only 44% identical to PDZ^3 domain (Fig. 2 *d*). Further evidence for the existence of a modular organization within PDZ domains of hDlg is provided by the fact that the proteolysis by three distinct proteolytic enzymes produced a remarkably similar pattern of protease-resistant PDZ domains. The compactness of the folded conformation of PDZ^{1+2} module is also indicated by the fact that the module resists further proteolysis despite the presence of 21 predicted cleavage sites of Asp-N, 26 cleavage sites of trypsin, and 14 cleavage sites of chymotrypsin within the module. Indeed, a high sequence identity and striking similarity in the proximal location of three PDZ domains found in hDlg, *Drosophila* Dlg, and PSD-95/SAP90 suggests that a similar modular organization of PDZ domains may also exist in other MAGUKs.

The use of proteases as a tool to delineate conformationally stable organization of protein domains has been successfully demonstrated in many cytoskeletal proteins. For example, the expression and crystallization of a 106–

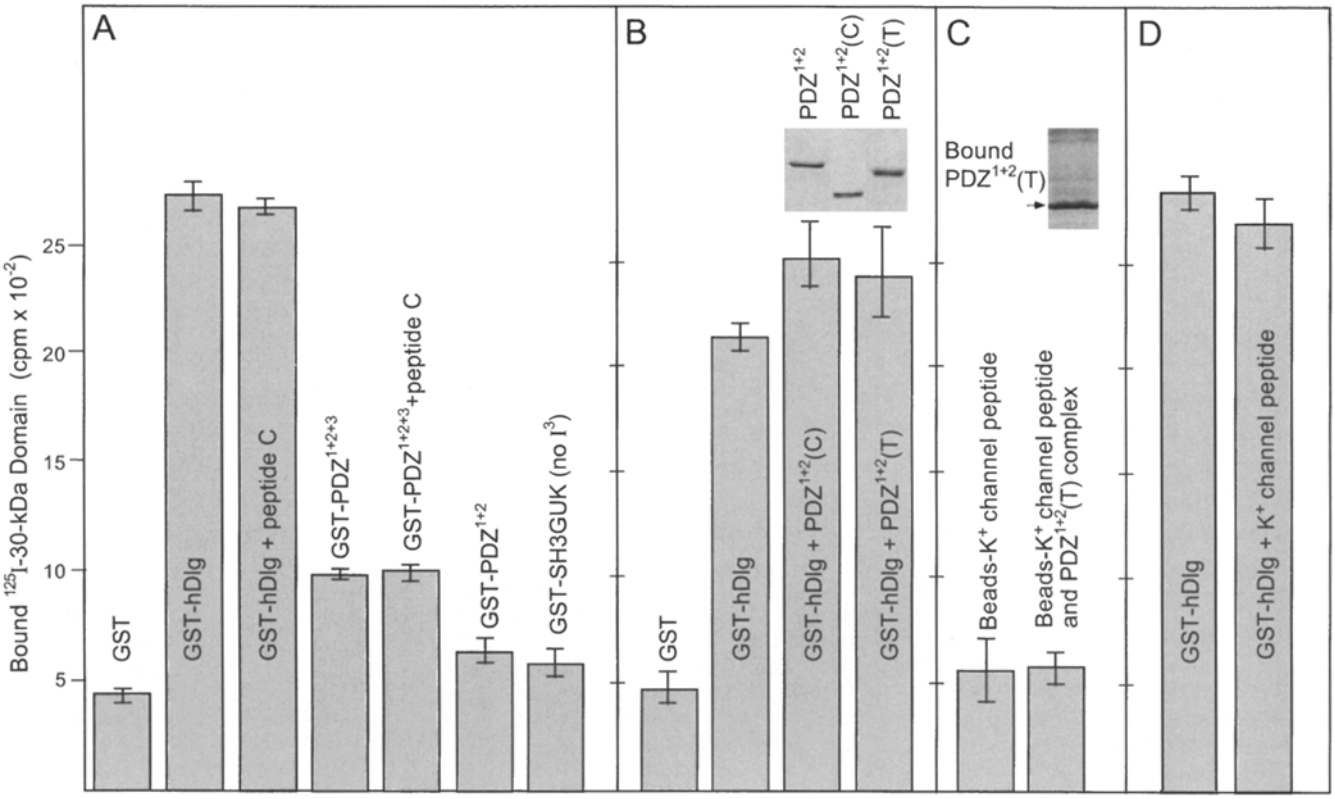

Figure 7. Binding of the 30-kD domain of protein 4.1 (4.1^{N30}) with recombinant hDlg proteins. The details of the sedimentation assay have been previously described (Marfatia et al., 1994). (*A*) ^{125}I-4.1^{N30} domain was incubated with beads containing either GST–hDlg protein or GST–PDZ^{1+2+3} domain, or GST–PDZ^{1+2} or GST–SH3+GUK domain. 20 M excess of peptide C was used to compete the binding of ^{125}I-4.1^{N30} domain to GST fusion proteins. The peptide C contains a positively charged amino acid cluster located between PDZ^1 and PDZ^2 domains of hDlg. The GST–PDZ^{1+2+3} protein sedimented 38% of ^{125}I-4.1^{N30} domain as compared with the full-length GST–hDlg protein. No binding of ^{125}I-4.1^{N30} domain was observed with either GST, GST–SH3+ GUK, or GST–PDZ^{1+2} proteins. Note that the SH3+GUK construct does not contain the 4.1B (I^3) insertion. (*B*) Binding of ^{125}I-4.1^{N30} domain of protein 4.1 with GST–hDlg protein in presence of PDZ^{1+2} (C) and PDZ^{1+2} (T) modules. The details for the production of PDZ^{1+2}, PDZ^{1+2} (C), and PDZ^{1+2} (T) are described in Materials and Methods. The SDS-PAGE analysis of purified proteins is shown in the inset. (*C*) Lack of binding of ^{125}I-4.1^{N30} domain to PDZ^{1+2} (T) module of hDlg. The PDZ^{1+2} module was incubated with streptavidin–agarose beads containing the biotinylated Kv1.4 peptide. (*Inset*) Amount and integrity of PDZ^{1+2} (T) module bound to the beads. The Kv1.4 peptide bound to the streptavidin beads was used as a control. No binding of ^{125}I-4.1^{N30} domain was detected with the PDZ^{1+2} (T) module. (*D*) Effect of Kv1.4 channel peptide on the binding of GST–hDlg with the ^{125}I-4.1^{N30} domain of protein 4.1. The GST–hDlg protein was incubated with 20 M excess of Kv1.4 channel peptide before the incubation with ^{125}I-4.1^{N30} domain of protein 4.1. The results are representative of three experiments carried out in duplicate or in triplicate. The values are a mean ± SEM (n = 2/3).

amino acid repeat unit of the *Drosophila* spectrin became feasible from studies of the boundaries of repeat units determined by protease digestion studies (Yan et al., 1993). A similar strategy has been used to show that the 24 ankyrin repeats are organized into four conformationally stable units in ankyrin (Michaely and Bennett, 1993). The organization of PDZ 1 and 2 domains into a distinct module readily explains the presence of either one or three PDZ domains in different MAGUKs. The PDZ^{1+2} module appears to mediate attachment to transmembrane proteins, explaining the submembrane localization of the large MAGUKs. The function of PDZ^3 domain, or single PDZ domain of the smaller MAGUKs, remains to be elucidated.

The results shown in Figs. 3 and 4 establish that a subset of PDZ domains are ATP-binding protein modules. Our data on ATP–PDZ binding for hDlg and Dlg appear to be consistent with the recent demonstration of ATP binding to full-length PSD-95/SAP90 (Kistner et al., 1995). Although the actual binding site on PSD-95 has yet to be mapped, it is unlikely to be the guanylate kinase domain because of a three–amino acid deletion in the putative ATP-binding motif (Woods and Bryant, 1993). In searching for a consensus nucleotide-binding sequence in the PDZ domains, we found that each of the three PDZ domains of hDlg as well as Dlg and PSD-95, contain a common "reverse" nucleotide-binding motif (**K/R**GXXGXG) at their amino termini (Figs. 2 and 10) (Saraste et al., 1990). Within the PDZ^{1+2} module of hDlg, the PDZ^1 domain contains an **R**GXXGXG signature, whereas the PDZ^2 domain carries a **K**GXXGXG. Likewise, PDZ domains 1 and 2 of Dlg and PSD-95 express the identical distribution of arginine and lysine. The PDZ^3 domain, however, varies slightly among the proteins; in hDlg and PSD-95, it contains **R**GXXGXG, while in Dlg, it has **K**GXXGXG (Figs. 2 and 10). Minor discrepancy notwithstanding, we

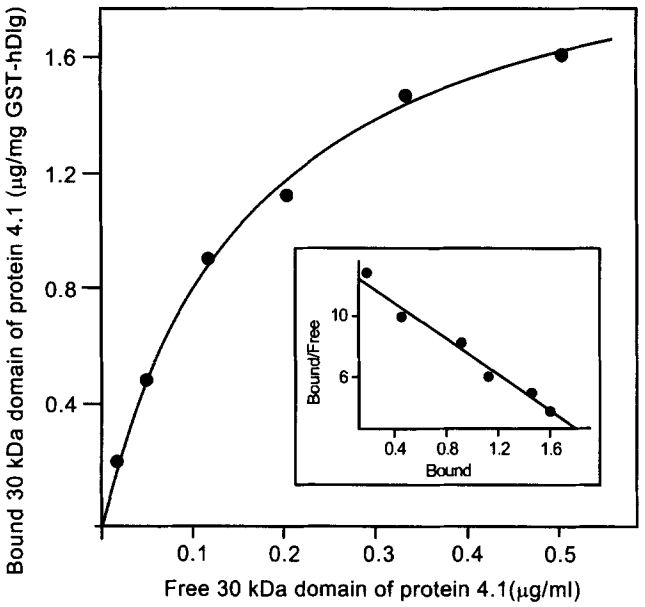

Figure 8. Quantification of the binding of GST–hDlg with the ^{125}I–30-kD domain of protein 4.1 (4.1^{N30}). The GST–hDlg binding data were plotted after subtraction of the GST background. (*Inset*) Scatchard analysis of the binding data. K_d = 5.3 ± 0.4 nM. The Scatchard analysis indicates the presence of a single class of high affinity protein 4.1–binding sites on hDlg. Each point is an average of duplicate determinations that were within 8% of experimental variation.

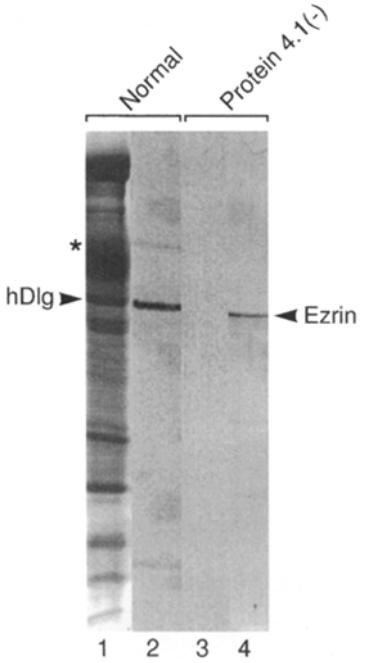

Figure 9. In vivo evidence for the association of hDlg with protein 4.1. Detection of hDlg protein in the membranes of elliptocytic RBCs. (*Arrowhead*) Position of the major 80-kD band of hDlg. (*Asterisk*) Mobility of the minor ~125-kD band of hDlg. The affinity-purified anti-peptide polyclonal antibodies were used to detect the presence of hDlg in the red cell membranes. (Lane *1*) Coomassie blue staining of normal red cell ghosts. (Lane *2*) hDlg Western blot of normal red cell ghosts. (Lane *3*) hDlg Western blot of 4.1 (−) HE ghosts. (Lane *4*) Ezrin Western blot of 4.1 (−) HE ghosts. Since a quantitative ELISA is not yet available, the determination of the number of copies of hDlg in the red cell membrane was not feasible at this stage. Note that the presence of ezrin has been previously demonstrated in the chicken RBCs (Winckler et al., 1994).

feel this motif may play a role in mediating ATP binding to PDZ domains. Although this consensus sequence is lacking in human erythroid p55's single PDZ domain and tight junction proteins ZO-1 and ZO-2's multiple PDZ domains, it must be acknowledged that no firm P-loop consensus sequence exists that can identify all ATP- or GTP-binding proteins. For example, phosphoglycerate kinases, which are known to bind ATP, exhibit a significantly divergent variation of the P-loop primary structure (Saraste et al., 1990). Thus, the absence of a classical P-loop consensus in some PDZ domains does not necessarily imply a lack of nucleotide binding.

The crystal structure of the PDZ^3 domain of PSD-95 complexed with peptide was recently solved by Doyle et al. (1996). They identified the peptide-binding interface as consisting of a Gly-Leu-Gly-Phe loop and an arginine-318. This model is similar to hDlg's PDZ^3 structure, in which a groove ending in a hydrophobic pocket and a buried arginine is also present and considered to be the binding site of peptide's COOH termini (Cabral et al., 1996). In light of the fact that hDlg and PSD-95 also share identical reverse nucleotide-binding motifs, it therefore appears unlikely that both ATP and peptide can bind to the same site on the PDZ^3 domain of hDlg and PSD-95. This prediction is in fact consistent with the lack of ATP binding to the PDZ^3 domain of hDlg (Fig. 3 *B*). The PDZ^3 domain of Dlg, in contrast, substitutes Lys-Gly-Pro for Arg-Gly-Ser in the reverse motif and may provide an additional site for nucleotide binding. Indeed, a GST–PDZ^3 fusion protein of Dlg binds ATP in vitro (data not shown), and the presence of a lysine residue in the P-loop has been previously proven critical in forming the dinucleotide fold necessary for nucleotide binding (Saraste et al., 1990). This Lys-Gly-Pro signature in Dlg's PDZ^3 domain is also present in the PDZ^2 domains of hDlg and PSD-95, which in conjunction with their corresponding PDZ^1 domains bind ATP. Whether this precise signature plays the key role in binding ATP to PDZ^{1+2} remains to be seen. Alternatively, there are several positively charged residues that could also serve as potential sites for ATP binding within the PDZ domains. Experiments are currently underway to solve the crystal structure of PDZ^{1+2} domain of hDlg in the presence of bound peptide and ATP.

Although the molecular mechanism by which MAGUKs function in vivo is not known, it is believed that they modulate signaling pathways at the membrane cytoskeleton (Woods and Bryant, 1993; Marfatia et al., 1995). The binding of ATP to the PDZ domains may have several important functional implications. First, in a subset of MAGUKs, the guanylate kinase domain shows a defective ATP-binding site (Woods and Bryant, 1993). The binding of ATP to PDZ domains may bring an ATP molecule in proximity to the guanylate kinase domain, thus making catalysis possible. Second, the hydrolysis of bound ATP may also induce conformational changes in MAGUKs, such as those seen in the nucleotide-bound forms of the ras oncoprotein (Al-

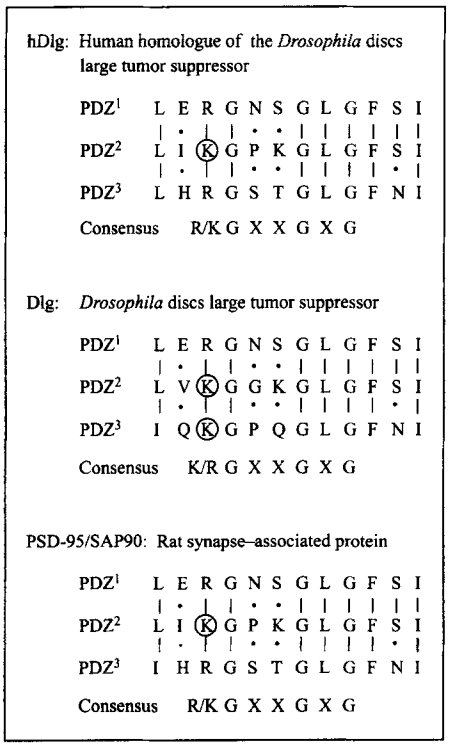

Figure 10. A comparison of the putative "reverse" nucleotide-binding sequence in the three PDZ domains of hDlg, Dlg, and PSD-95/SAP90. The consensus sequence is shown at the bottom of each panel. Note that this region is also identified as the peptide-binding site in the PDZ^3 domain of PSD-95/SAP90 (Doyle et al., 1996).

berts and Miake-Lye, 1992). Third, binding of ATP by the PDZ domains may indirectly affect the functions of other proteins with which MAGUKs interact.

Using a yeast two-hybrid screen, Kim et al. (1995) have recently shown an interaction between the carboxyl terminus of the Kv1.4 channel and PDZ domains 1 and 2 of the PSD-95 protein. They have also shown an interaction between the cytoplasmic domain of Kv1.4 channel and a construct of the hDlg protein that contains three PDZ domains and an SH3 motif (Kim et al., 1995). In this paper, we have shown that the PDZ domains 1 and 2 of hDlg contain the binding site for the cytoplasmic domain of Shaker-type K^+ channels (Figs. 5 and 6). The cytoplasmic domain of Shaker-type K^+ channels does not contain a consensus nucleotide-binding sequence (Chandy and Gutman, 1995). Therefore, the binding of the PDZ^{1+2} module of hDlg to ATP provides a molecular framework by which K^+ channels could be coupled to ATP via the PDZ^{1+2} module of hDlg. The coupling of K^+ channels to metabolic energy may have profound consequences for the functioning of these channels in the cell. The carboxyl terminus plays a critical role in determining the inactivation gating of K^+ channels (Isacoff et al., 1990), and such inactivation events may be coupled to the hydrolysis of ATP bound to the PDZ^{1+2} module of hDlg. Alternatively, the homotypic and heterotypic associations of K^+ channels may be modulated by the interaction of their carboxyl termini with the PDZ^{1+2} module of hDlg (Xu et al., 1995; Fig. 11). Such interactions may then be subject to regulation by the hydrolysis of ATP bound to the PDZ^{1+2} module of hDlg. Many precedents exist in which protein-bound nucleotides play a critical role in regulating the functions of proteins such as in myosin, kinesin, dyneins, ras, heat shock protein 70, and CFTR (Alberts and Miake-Lye, 1992; Gilbert et al., 1995). Cytosolic ATP has been shown to inhibit the function of at least one kind of K^+ channel, K_{ATP} (Philipson, 1995). The hDlg protein could also play a role in the activation of T lymphocytes via K^+ channels. The mitogenic activation of murine T lymphocytes results in a 20-fold increase in the Kv1.3 current density (Cahalan et al., 1987; Deutsch, 1990). Whether the hDlg and its bound ATP participate in such mitogenesis-induced K^+ current fluctuations in lymphocytes remains to be determined.

Our results show that protein 4.1 binds to hDlg at a single site encoded by an alternatively spliced exon located between the SH3 and guanylate kinase homologous domains. Although the data in Fig. 7 *A* showing a weak interaction between the GST–PDZ^{1+2+3} fusion protein and protein 4.1 are consistent with our previous findings (Lue et al., 1994), it appears that the protein 4.1 binding to the PDZ domains is an artifactual consequence of a cluster of positively charged residues present at the interface of PDZ domains 1 and 2. We have used several complementary approaches to demonstrate that this is indeed the case. (*a*) The PDZ^{1+2} module of hDlg does not bind to protein 4.1 (Fig. 8 *A*) and does not compete with the binding of full-length hDlg to protein 4.1 (Fig. 7 *B*). (*b*) A synthetic peptide (peptide C), which includes the positively charged amino acids located between the PDZ domains 1 and 2, fails to inhibit the binding of protein 4.1 to hDlg and PDZ^{1+2+3} in vitro (Fig. 8 *A*). (*c*) The binding of Kv1.4 peptide to the PDZ^{1+2} module does not modulate its binding to protein 4.1 (Fig. 7 *C*). (*d*) Finally, Scatchard analysis of the binding data clearly shows that protein 4.1 binds to hDlg at a single high affinity site (Fig. 8).

The results shown in Fig. 9 provide the first evidence for

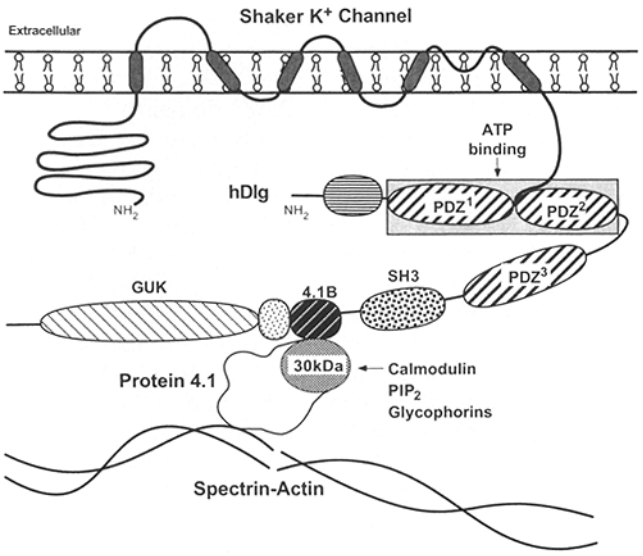

Figure 11. A model showing the coupling of K^+ channel (Kv1.4) to ATP and cytoskeleton via the PDZ domains of hDlg. Note that the 30-kD domain of protein 4.1 (4.1^{N30}) also binds to effector molecules such as calmodulin and phospholipids.

an in vivo interaction between protein 4.1 and hDlg, by demonstrating the absence of hDlg protein from the RBC membranes of a patient with homozygous protein 4.1 (−) hereditary elliptocytosis. The secondary loss of both hDlg and p55 in the membranes of these naturally mutant RBCs underscores the importance of protein 4.1 as an attachment molecule for hDlg and p55 at the plasma membrane. The data in this paper also indicate that the hDlg protein does not bind to at least some members of the protein 4.1 superfamily such as ezrin and PTP-H1 tyrosine phosphatase. The presence of ezrin in the membranes of protein 4.1 (−) HE RBCs confirms that hDlg and p55 do not directly interact with ezrin in the red cell membrane (Fig. 9).

A recent study has shown that the three PDZ domains of hDlg are organized into two protease-resistant domains (Lue, R.A., E. Brandin, E.P. Chan, and D. Brandon. 1995. *Mol. Biol. Cell. (Suppl.)*. Vol. 6. Abstract #1557). Although the precise boundaries of the domains were not determined, the results are in agreement with our studies of organization of PDZ domains (Fig. 1). In the same study, it was shown that protein 4.1 binds to a protease-resistant module of hDlg containing PDZ domains 1 and 2 (Lue et al., 1995 [Abstract #1557], as cited above). In contrast, our results show that protein 4.1 does not bind to the PDZ^{1+2} module that contains PDZ domains 1 and 2 of hDlg (Fig. 7). At this stage, we do not know the reason for this discrepancy. In any case, the data in this paper clearly show that the protein 4.1–binding site is located between the SH3 and guanylate kinase domains of hDlg. It is noteworthy that a remarkably conserved protein 4.1–binding site exists between the SH3 and guanylate kinase domains of other MAGUKs including Dlg and PDS-95/SAP90. Whether protein 4.1 or members of the protein 4.1 superfamily bind to Dlg and PSD-95 remains to be determined.

The functional significance of the binding of protein 4.1 to MAGUKs is unclear at present. It is clear from recent studies that the cytoplasmic domain of transmembrane channels mediates their clustering at the interface of membrane–cytoskeleton (Kim et al., 1995). However, the mechanism of such clustering remains unknown. Our results raise the possibility that the clustering of transmembrane channels may be mediated via their interactions with protein 4.1. Another possibility is that the K^+ channels and other PDZ domain–binding proteins may be coupled to effector molecules such as calmodulin and phosphoinositides via the 30-kD domain (4.1^{N30}) of protein 4.1 (Fig. 11). Whether the binding of ATP to the PDZ^{1+2} module of hDlg can functionally modulate properties of the K^+ channels such as their membrane clustering and interactions with the cytoskeleton remains to be determined. If true, a similar molecular mechanism may also be invoked for the interactions of transmembrane *N*-methyl-D-aspartate receptors, K^+ channels, and adenomatous polyposis coli gene product that bind to the PDZ^2 domain of PSD-95/SAP90 and hDlg, respectively (Kornau et al., 1995; Kim et al., 1995; Matsumine et al., 1996). Such queries are now amenable to experimental testing by using mutant forms of hDlg and PSD-95/SAP-90 proteins, and by assessing their effects on the properties of PDZ domain–binding proteins in heterologous expression systems.

We thank Dr. Jim LaDine of the FISONS IAsys (New Jersey) for measuring the interaction of potassium channel peptide with the PDZ^{1+2} module of hDlg; Dr. Anthony Bretscher (Cornell University) for providing purified ezrin protein and antibodies; and Ms. Laura Derick for help with EM of PDZ domains. We also thank Ms. Donna-Marie Mironchuk and Mr. Andrew Geffken for help with the preparation of this manuscript.

This work was supported by the National Institutes of Health grants CA66263 and HL 51445. S.M. Marfatia is supported by the Young Investigator award from the National Neurofibromatosis Foundation. A.H. Chishti is an established investigator of the American Heart Association.

Received for publication 2 May 1996 and in revised form 16 August 1996.

References

Alberts, B., and R. Miake-Lye. 1992. Unscrambling the puzzle of biological machines: the importance of the details. *Cell.* 68:415–420.

Alloisio, N., N.D. Venezia, A. Rana, K. Andrabi, P. Texier, F. Gilsanz, J.P. Cartron, J. Delaunay, and A.H. Chishti. 1993. Evidence that red blood cell protein p55 may participate in the skeleton-membrane linkage that involves protein 4.1 and glycophorin C. *Blood.* 82:1323–1327.

Azim, A.C., J.H.M. Knoll, S.M. Marfatia, D.J. Peel, P.J. Bryant, and A.H. Chishti. 1995. DLG1: chromosome location of the closest human homologue of the *Drosophila discs large* tumor suppressor gene. *Genomics.* 30:613–616.

Azim, A.C., S.M. Marfatia, C. Korsgren, E. Dotimas, C.M. Cohen, and A.H. Chishti. 1996. Human erythrocyte dematin and protein 4.2 (Pallidin) are ATP binding proteins. *Biochemistry.* 35:3001–3006.

Brenman, J.E., D.S. Chao, S.H. Gee, A.W. McGee, S.E. Craven, D.R. Santillano, Z. Wu, F. Huang, H. Xia, M.F. Peters et al. 1996. Interaction of nitric oxide synthase with the postsynaptic density protein PSD-95 and α1syntrophin mediated by PDZ domains. *Cell.* 84:757–767.

Cabral, J.H.M., C. Petosa, M.J. Sutcliffe, S. Raza, O. Byron, F. Poy, S.M. Marfatia, A.H. Chishti, and R.C. Liddington. 1996. Crystal structure of a PDZ domain from the human homologue of discs-large protein. *Nature (Lond.).* 382: 649–652.

Cahalan, M.D., K.G. Chandy, T.E. DeCoursey, S. Gupta, R.S. Lewis, and J.B. Sutro. 1987. *In* Mechanisms of Lymphocyte Activation and Immune Regulation. S. Gupta, W.E. Paul, and A.S. Fauci, editors. Plenum, New York. 85–101.

Chandy, K.G., and G. A. Gutman. 1995. Voltage-gated K^+ channel genes. *In* Handbook of Receptors and Channels: Ligands and Voltage-gated Ion Channels. A. North, editor. CRC Press, Boca Raton, FL. 1–71.

Chishti, A.H., J. Palek, D. Fisher, G.J. Maalouf, and S.-H. Liu. 1996. Reduced invasion and growth of *Plasmodium falciparum* into elliptocytic red blood cells with a combined deficiency of protein 4.1, glycophorin C, and p55. *Blood.* 87:3462–3469.

Cho, K., C.A. Hunt, and M.B. Kennedy. 1992. The rat brain postsynaptic density fraction contains a homolog of the *Drosophila* discs-large tumor suppressor protein. *Neuron.* 9:929–942.

Deutsch, C. 1990. Potassium Channels: Basic Function and Therapeutic Aspects. T.J. Colatsky, editor. Wiley-Liss, New York. 251–271.

Doyle, D.A., A. Lee, J. Lewis, E. Kim, M. Sheng, and R. MacKinnon. 1996. Crystal structures of a complexed and peptide-free membrane protein-binding domain: molecular basis of peptide recognition by PDZ. *Cell.* 85:1067–1076.

Feo, C.J., S. Fischer, J.P. Piau, M.J. Grange, and G. Tchernia. 1980. Premier observation de l'absence d'une proteine de la membrane erythrocytaire familiale. *Nouv. Rev. Fr. Hematol.* 22:315–325.

Gilbert, S.P., M.R. Webb, M. Brune, and K.A. Johnson. 1995. Pathway of processive ATP hydrolysis by kinesin. *Nature (Lond.).* 373:671–676.

Hata, Y., S. Butz, and T.C. Sudhof. 1996. CASK: a novel dlg/PSD95 homolog with an N-terminal calmodulin-dependent protein kinase domain identified by interaction with neurexins. *J. Neurosci.* 16:2488–2494.

Hoskins, R., A.F. Hajnal, S.A. Harp, and S.K. Kim. 1996. The *C. elegans* vulval induction gene *lin-2* encodes a member of the MAGUK family of cell junction proteins. *Development (Camb.).* 122:97–111.

Isacoff, E., D. Papazian, L. Timpe, Y.-N. Jan, and L.-Y. Jan. 1990. Molecular studies of voltage-gated potassium channels. *Cold Spring Harbor Symp. Quant. Biol.* 55:9–17.

Itoh, M., A. Nagafuchi, S. Yonemura, T. Kitani-Yasuda, S. Tsukita, and S. Tsukita. 1993. The 220-kD protein colocalizing with cadherins in non-epithelial cells is identical to ZO-1, a tight junction–associated protein in epithelial cells: cDNA cloning and immunoelectron microscopy. *J. Cell Biol.* 121:491–502.

Jesaitis, L.A., and D.A. Goodenough. 1994. Molecular characterization and tissue distribution of ZO-2, a tight junction protein homologous to ZO-1 and the *Drosophila* discs-large tumor suppressor protein. *J. Cell Biol.* 124:949–961.

Kim, E., A.R. Niethammer, A. Rothschild, Y.N. Jan, and M. Sheng. 1995. Clustering of Shaker-type K^+ channels by direct interaction with the PSD-95/SAP90 family of membrane-associated guanylate kinases. *Nature (Lond.).* 378:85–88.

Kistner, U., B.M. Wenzel, R.W. Veh, C. Cases-Langhoff, A.M. Garner, U. Appeltauer, B. Voss, E.D. Gundelfinger, and C.C. Garner. 1993. SAP90, a rat presynaptic protein related to the product of the *Drosophila* tumor suppres-

sor gene dlg-A. *J. Biol. Chem.* 268:4580–4583.
Kistner, U., C.C. Garner, and M. Linial. 1995. Nucleotide binding by the synapse associated protein SAP90. *FEBS Lett.* 359:159–163.
Klingensmith, J., R. Nusse, and N. Perrimon. 1993. The *Drosophila* segment polarity gene dishevelled encodes a novel protein required for response to wingless signal. *Genes & Dev.* 8:118–130.
Kornau, H.-C., L.T. Schenker, M.B. Kennedy, and P.H. Seeburg. 1995. Domain interaction between NMDA receptor subunits and the postsynaptic density protein PSD-95. *Science (Wash. DC).* 269:1737–1740.
Ling, E., Y.N. Danilov, and C.M. Cohen. 1988. Modulation of red cell band 4.1 function by cAMP-dependent kinase and protein kinase C phosphorylation. *J. Biol. Chem.* 263:2209–2216.
Lue, R.A., S.M. Marfatia, D. Branton, and A.H. Chishti. 1994. Cloning and characterization of hdlg: the human homologue of the *Drosophila* discs large tumor suppressor binds to protein 4.1. *Proc. Natl. Acad. Sci. USA.* 91:9818–9822.
Marfatia, S.M., R.A. Lue, D. Branton, and A.H. Chishti. 1994. In vitro binding studies suggest a membrane-associated complex between erythroid p55, protein 4.1, and glycophorin C. *J. Biol. Chem.* 269:8631–8634.
Marfatia, S.M., R.A. Lue, D. Branton, and A.H. Chishti. 1995. Identification of the protein 4.1 binding interface on glycophorin C and p55, a homologue of the *Drosophila* discs-large tumor suppressor protein. *J. Biol. Chem.* 270:715–719.
Matsumine, A., A. Ogai, T. Senda, T. Okumure, S. Kobayashi, M. Okada, K. Toyoshima, and T. Akiyama, T. 1996. Binding of APC to the human homolog of the *Drosophila* discs large tumor suppressor protein. *Science (Wash. DC).* 272:1020–1026.
Mazoyer, S., S.A. Gayther, M.A. Nagai, S.A. Smith, A. Dunning, E.J. van Rensburg, H. Albertsen, R. White, and B.A.J. Ponder. 1995. A gene (DLG2) located at 17q12-q21 encodes a new homologue of the Drosophila tumor suppressor dlg-A. *Genomics.* 28:25–31.
Michaely, P., and V. Bennett. 1993. The membrane-binding domain of ankyrin contains four independently folded subdomains, each comprised of six ankyrin repeats. *J. Biol. Chem.* 268:22703–22709.
Müller, B.M., U. Kistner, R.W. Veh, C. Cases-Langhoff, B. Becker, E.D. Gundelfinger, and C.C. Garner. 1995. Molecular characterization and spatial distribution of SAP97, a novel presynaptic protein homologous to SAP90 and the *Drosophila* discs-large tumor suppressor protein. *J. Neurosci.* 15:2354–2366.
Ohanian, V., and W. Gratzer. 1984. Preparation of red-cell-membrane cytoskeletal constituents and characterisation of protein 4.1. *Eur. J. Biochem.* 144: 375–379.
Pelham, H.R.B., and R.J. Jackson. 1976. An efficient mRNA-dependent translation system from reticulocyte lysates. *Eur. J. Biochem.* 67:247–256.
Phillipson, L.H. 1995. ATP-sensitive K^+ channels: paradigm lost, paradigm regained. *Science (Wash. DC).* 270:1159.
Ponting, C.P., and C. Phillips. 1995. DHR domains in syntrophins, neuronal NO synthases and other intracellular proteins. *Trends Biochem. Sci.* 20:102–103.
Ruff, P., D.W. Speicher, and A.H. Chishti. 1991. Molecular identification of a major palmitoylated erythrocyte membrane protein containing the src homology 3 motif. *Proc. Natl. Acad. Sci. USA.* 88:6595–6599.
Saraste, M., P.R. Sibbald, and A. Wittinghofer. 1990. The P-loop—a common motif in ATP- and GTP-binding proteins. *Trends Biochem. Sci.* 15:430–434.
Sato, T., S. Irie, S. Kitada, and J.C. Reed. 1995. FAP-1: a protein tyrosine phosphatase that associates with Fas. *Science (Wash. DC).* 268:411–415.
Simske, J.S., S.M. Kaech, S.A. Harp, and S.K. Kim. 1996. LET-23 receptor localization by the cell junction protein LIN-7 during *C. elegans* vulval induction. *Cell.* 85:195–204.
Smith, D.B., and K.S. Johnson. 1988. Single-step purification of polypeptides expressed in *Escherichia coli* as fusions with glutathione S-transferase. *Gene (Amst.).* 67:31–40.
Smith, S.A., P. Holik, J. Stevens, S. Mazoyer, R. Melis, B. Williams, R. White, and H. Albertsen. 1996. Isolation of a gene (DLG3) encoding a second member of the discs-large family on chromosome 17q12-q21. *Genomics.* 31: 145–150.
Tyler, J.M., B. N. Reinhardt, and D. Branton. 1980. Associations of erythrocyte membrane proteins. Binding of purified band 2.1 and 4.1 to spectrin. *J. Biol. Chem.* 255:7034–7039.
Willott, E., M.S. Balda, A.S. Fanning, B. Jameson, C.V. Itallie, and J.M. Anderson. 1993. The tight junction protein ZO-1 is homologous to the *Drosophila* discs-large tumor suppressor protein of septate junctions. *Proc. Natl. Acad. Sci. USA.* 90:7834–7838.
Winckler, B., A.C. Gonzalez, M. Magendantz, and F. Solomon. 1994. Analysis of a cortical cytoskeletal structure: role for ezrin-radixin-moesin (ERM proteins) in the marginal band of chicken erythrocytes. *J. Cell Sci.* 107:2523–2534.
Woods, D.F., and P.J. Bryant. 1991. The discs-large tumor suppressor gene of *Drosophila* encodes a guanylate kinase homolog localized at septate junctions. *Cell.* 66:451–464.
Woods, D.F., and P.J. Bryant. 1993. ZO-1, DlgA and PSD-95/SAP90: homologous proteins in tight, septate and synaptic cell junctions. *Mech. Dev.* 44:85–89.
Xu, J., W. Yu, Y.N. Jan, L.Y. Jan, and M. Li. 1995. Assembly of voltage-gated potassium channels. Conserved hydrophilic motifs determine subfamily-specific interactions between the α-subunits. *J. Biol. Chem.* 270:24761–24768.
Yan, Y., E. Winograd, A. Viel, T. Cronin, S.C. Harrison, and D. Branton. 1993. Crystal structure of the repetitive segments of spectrin. *Science (Wash. DC).* 262:2027–2030.
Yanagawa, S., F. Leeuwen, A. Wodarz, J. Klingensmith, and R. Nusse. 1995. The dishevelled protein is modified by wingless signaling in *Drosophila*. *Genes & Dev.* 9:1087–1097.